CCC 2008 - Challenges for Civil Construction
Torres Marques et al. (Eds)

ANALYTICAL MODELLING STRATEGY FOR PREDICTING THE NSM FRP STRIPS CONTRIBUTION TO RC BEAMS SHEAR STRENGTH

Vincenzo Bianco[*], Joaquim A.O. Barros[†] and Giorgio Monti[*]

[*] Dept. of Structural Engrg. and Geotechnics
University Sapienza of Rome
Via Gramsci 53, 00197 Rome, Italy
e-mail: giorgio.monti@uniroma1.it, web page: http://www.disg.uniroma1.it

[†] ISISE, Department of Civil Engineering
Universidade do Minho
Campus de Azurém, 4800-058 Guimarães, Portugal
e-mail: barros@civil.uminho.pt, web page: http:// www.civil.uminho.pt/composites

Keywords: FRP reinforcement, shear strengthening, debonding, concrete semi-conical fracture, strip tensile rupture.

Summary: *Shear strengthening of RC beams by means of FRP strips glued by a structural adhesive into thin shallow slits cut in the cover of the web lateral faces, is becoming a popular technique. Nonetheless, many aspects related to the mechanical behaviour and relevant failure modes still need to be clarified. A recent experimental-analytical investigation has demonstrated that, besides debonding and tensile rupture of the strip, the semi-conical tensile fracture of concrete surrounding the strip should be considered among the possible failure modes. A comprehensive analytical model for predicting the NSM strips contribution to the shear strength of RC beams was also developed. Despite its consistency with experimental results, that model had room for improvements. The upgraded version of that analytical model is herein presented and appraised on the basis of some among the most recent experimental results. This appraisal shows the high level of accuracy and potentialities of that modelling strategy arise.*

1 INTRODUCTION

Some among the most recent experimental works [1,2] devoted at appraising the potentialities of the technique of Near Surface Mounted (NSM) CFRP strips for shear strengthening of RC beams spotlighted the occurrence of a failure mode consisting of the progressive detachment of the concrete cover from the underlying core of the beam. That peculiar failure mode was even more pronounced in the case of low strength concrete beams [3]. A subsequent analytical investigation [4] demonstrated that such failure mode can be ascribed to the "semi-conical" tensile fracture of concrete surrounding each NSM strip. When the principal tensile stresses transferred to the surrounding concrete exceed its tensile strength, concrete fractures along the surface envelope of the compression isostatics, whose shape can be conveniently assumed as semi-conical.

An analytical predictive model was subsequently developed [5,6] for predicting the NSM strips' shear strength contribution. That model assumed as possible failure modes affecting the behaviour, at ultimate, of the NSM strips: debonding, concrete tensile fracture and tensile rupture of the strip itself. It resulted innovative, not only for bringing in a new failure mode, neglected up to that moment, but also for allowing the interaction among adjacent strips to be easily accounted for, and quantified. In that occasion, the modelling strategy adopted to simulate and to quantify the NSM strips' capacity attributable to semi-conical concrete tensile fracture was developed in closed form, resulting as robust and rational. On the contrary, the modelling strategy adopted for predicting the debonding-dependent

capacity of a single NSM strip was based on analytical relationships obtained from experimental data regression. That part of the model resulted, in that way, not scientifically rigorous and susceptible of improvements.

Moreover, in that occasion, the interaction between the force transfer mechanism from the strip to the surrounding concrete by bond, and the progressive formation of semi-conical fracture surfaces had not been addressed in depth, yet. The further investigation of that interaction has spotlighted that another failure mode has to be considered, among those affecting the behaviour at ultimate of an NSM strip, composed of a concrete shallow semi-cone tensile fracture plus debonding (Fig. 1d).

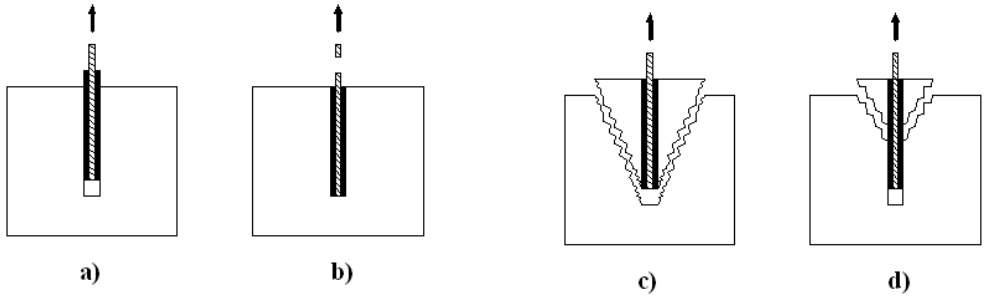

a) b)

Figure 1: Possible failure modes of an NSM FRP strip: a) debonding; b) strip tensile rupture; c) concrete semi-conical tensile fracture; d) mixed shallow semi-cone plus debonding.

That analytical model also needed to be improved by introducing kinematic compatibility, since it had originally assumed that all of the strips reach their ultimate state simultaneously, which is not the case of a system of FRPs bridging a shear crack [7].

In the present work, the main ideas behind the algorithm employed to implement the upgraded version of that model, together with the main findings, are presented. For the sake of brevity, all of the analytical details are herein omitted, but they can be found elsewhere [8].

2 SHEAR STRENGTH CONTRIBUTION BY A SYSTEM OF NSM FRP STRIPS

2.1 Physical fundamentals and general algorithm

The developed analytical model aims at predicting the NSM FRP strips shear strength contribution. The algorithm adopted (Fig. 4), takes as input both geometrical and mechanical parameters *i.e.*: depth h_w and width b_w of the strengthened beam web; inclination of both the Critical Diagonal Crack (CDC) angle θ and strips angle β with respect to the beam longitudinal axis; strips' spacing measured along the beam axis s_f; angle α between axis and generatrices of the semi-conical fracture surface; concrete average compressive strength f_{cm}; strips tensile strength f_{fu} and Young's modulus E_f; thickness a_f and width b_f of the strip's cross section; values of bond stress τ_0, τ_1, τ_2 and slip $\delta_1, \delta_2, \delta_3$ defining the adopted local bond stress-slip relationship, as further specified hereafter; increment $\dot{\gamma}$ and maximum value $\gamma_{\max}$ of the opening angle of the CDC.

The local bond stress slip relationship, herein adopted [9] to simulate the different phases undergone in sequence by bond during the loading process, is composed of four linear branches (Fig. 2). Those phases, representing the physical phenomena occurring in sequence, within the adhesive layer by increasing the imposed end slip, are: "elastic", "softening", "softening friction" and "free slipping". The initial bond strength τ_0, independent of the adhesive layer deformability, is due to the micromechanical and chemical properties of the materials involved. The parameter τ_0 represents the

average of the following physical entities encountered in sequence by forces migrating from the strip to the surrounding concrete, which are: adhesion at the strip-adhesive interface, cohesion within the adhesive layer and adhesion at the adhesive-concrete interface. From τ_0 up to the peak strength τ_1, a macro-mechanical strength due to the adhesive layer elastic stiffness adds to the constant adhesive-cohesive strength. That macro-mechanical strength due to the elastic stiffness of the intact adhesive layer can be conveniently modeled by a linear elastic behavior. Approaching the peak strength, the adhesive fractures along diagonal planes orthogonal to the tensile isostatics [10]. During the subsequent softening phase, force is transferred from the strip to the surrounding concrete by the resulting diagonal micro-struts. Anyway, throughout the softening phase, by increasing the imposed slip, the adhesive at the extremities of those struts progressively deteriorates, so that, by increasing the imposed slip, micro-cracks parallel to the strip start to appear at both the strip-adhesive and adhesive-concrete interfaces. Approaching the softening friction phase, the softening resisting mechanism is gradually converted in friction and micro-mechanical interlock along those micro-cracks. Nonetheless, even those mechanisms undergo softening due to progressive degradation. When the resisting force provided by friction is exhausted, those micro-cracks result in smooth discontinuities. The free slipping phase follows, during which the strip keeps being pulled out without having to overcome any opposing restraint.

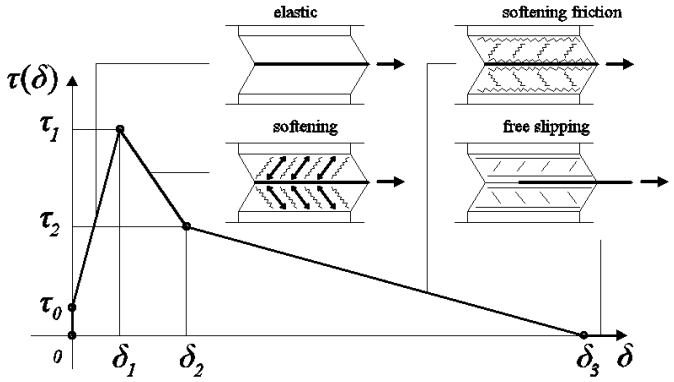

Figure 2: Adopted local bond stress-slip relationship.

During the loading process of a RC beam subject to shear, when the concrete average tensile strength f_{ctm} is overcome at the web intrados, some shear cracks originate therein and successively progress towards the web extrados. Those cracks can be thought of as a single Critical Diagonal Crack inclined of an angle θ with respect to the beam longitudinal axis (Fig. 3a). The CDC can be schematized as an inclined plane dividing the web into two portions sewn together by the crossing strips (Fig. 3b). At load step t_1, the two web parts separated by the CDC start moving apart by pivoting around the crack end (point E in Fig. 3a). From that step on, by increasing the applied load, the CDC opening angle $\gamma(t_n)$ progressively widens.

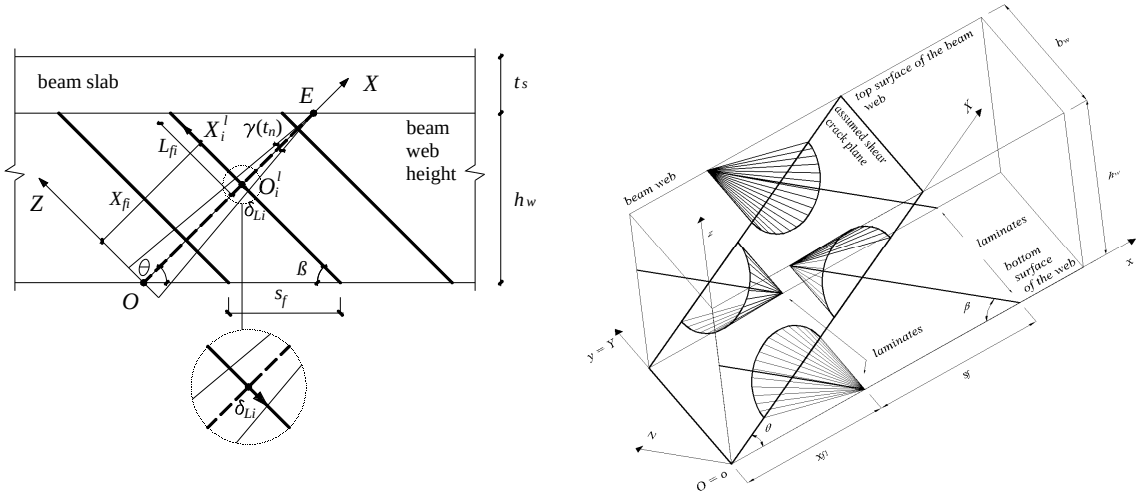

a) b)

Figure 3: RC beam strengthened in shear by NSM FRP strips: lateral (a) and axonometric view (b).

Strips crossing the crack, oppose its widening by anchoring to the surrounding concrete to which they transfer, by bond, force originating at their extremity O_i^l lying on the CDC due to the imposed end slip $\delta_{Li}\left[\gamma\left(t_n\right)\right]$. The capacity of each strip is the one provided by its available bond length L_{fi}, that is the shorter between the two parts on either side of the crack. At each load step $\gamma\left(t_n\right)$ the physical behaviour of the structural system including strips, adhesive and concrete is extremely complex. However, it can be easily explained if some simplifying assumptions are assumed, such as: large spacing between strips and perpendicularity between strips and CDC. The former is meant to exclude any interaction among the strips, thus allowing attention be focused on the i-th strip only (Fig. 5) and the latter imposes the semi-conical cracks to be orthogonal to the CDC plane, thus simplifying the evaluation of the concrete fracture capacity as further explained hereafter.

Three different possible geometrical configurations [5] assumed by the system of FRPs with respect to the CDC are singled out in order to determine the analytical range $\left[V_{f,\min};V_{f,\max}\right]$ of values of shear strength contribution provided by the NSM strips. Those three configurations, defined by the number of strips $N_{f,k}$ and position of the first strip $x_{f1,k}$ with respect to the CDC origin, are defined as follows: 1) the minimum number of strips with the first one located at a distance equal to the spacing; 2) an even number of strips symmetrically placed with respect to the crack axis; 3) an odd number of strips with the central one attaining the maximum length by being located along the crack axis.

For each load step $\gamma\left(t_n\right)$, and for each of the three geometrical configurations, the capacity of the single i-th strip parallel to its orientation $V_{fi,k}^{p}\left(\delta_{Li}\right)$, is evaluated as the minimum among the three terms $V_{fi,k}^{bd}$, V_f^{tr} and $V_{fi,k}^{cf}$, attributable to bond transfer, strip tensile rupture and concrete semi-conical tensile fracture, respectively. The last one, in the most general case in which the simplifying assumption of above are abandoned, and due to the interaction among adjacent strips, also depends on the available bond length along which concrete has fractured for all of the strips, up to that point.

The overall NSM strips shear strength contribution is then simply obtained by summation and projection on the direction orthogonal to the beam longitudinal axis, as follows:

$$V_{f,k}(\gamma) = 2 \cdot \sin\beta \cdot \sum_{i=1}^{N_{f,k}} V_{fi,k}^{p} \tag{1}$$

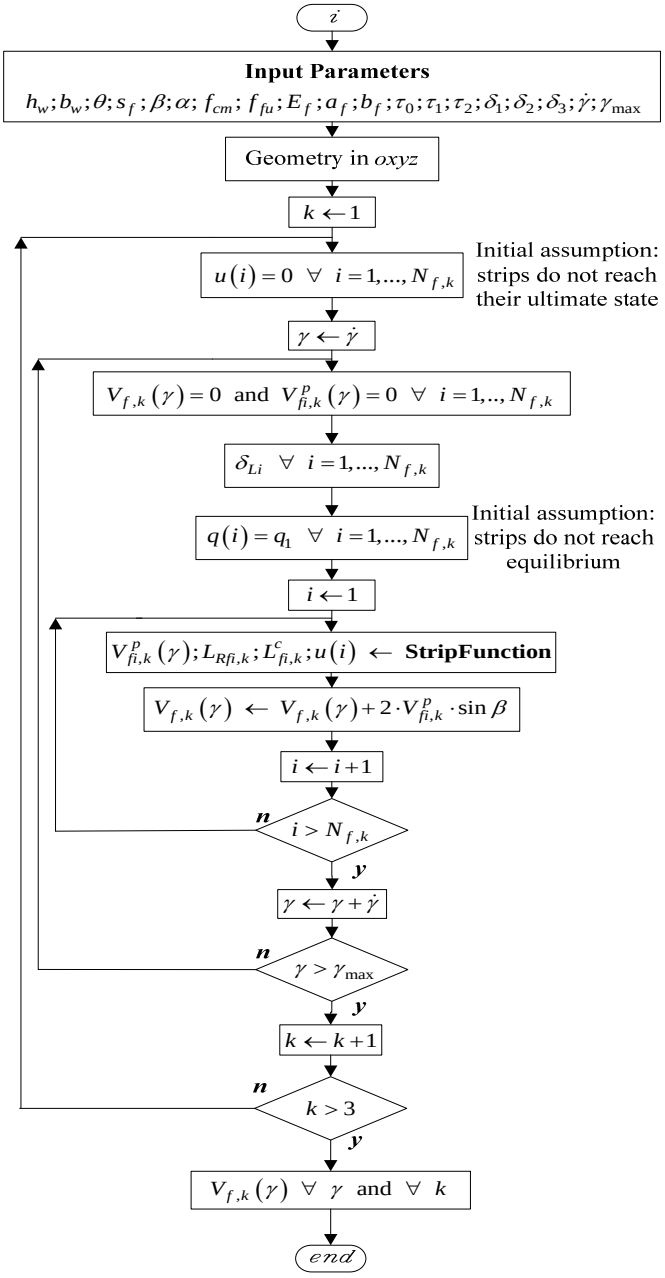

Figure 4: Flow chart of the algorithm.

2.2 Contribution of a single NSM FRP strip

The structural behaviour involving strip, adhesive and concrete, can be described by an iterative

process (Fig. 5) aiming at determining, for a given value of $\gamma(t_n)$, the state of equilibrium of the structural system. The n-th iteration is indicated by q_n ranging from q_1 (first iteration) to q_e (iteration in correspondence of which equilibrium is attained). In each iteration q_n, it is possible to define, for each i-th strip, the following quantities:

- $L_{Rfi}(t_n;q_n)$: the "resisting bond length", *i.e.*, the portion of L_{fi} still bonded to concrete;
- $L^c_{fi}(t_n;q_n)$: the "concrete semi-cone height", *i.e.*, the portion of L_{fi} around which the surrounding concrete has fractured along a semi conical surface;
- $L_{tr,i}\left[\delta_{Li}(t_n);L_{Rfi}(t_n;q_n)\right]$: the "transfer length", *i.e.*, the portion of L_{Rfi} along which the i-th strip transfers the corresponding bond force V^{bd}_{fi} to the surrounding concrete;
- $V^{bd}_{fi}\left[\delta_{Li}(t_n);L_{Rfi}(t_n;q_n);x^{tr}_i\right]$: the progressive value of the force transferred by bond to the surrounding concrete along $L_{tr,i}$, where x^{tr}_i is the reference axis along $L_{tr,i}$;
- $V^{bd}_{fi}\left[\delta_{Li}(t_n);L_{Rfi}(t_n;q_n)\right]$: the force transferred by bond to the surrounding concrete along $L_{tr,i}$, given by $V^{bd}_{fi}\left[\delta_{Li}(t_n);L_{Rfi}(t_n;q_n);L_{tr,i}\right]$.

When the i-th strip is subjected to the first imposed end slip $\delta_{Li}(t_1)$, the resulting force $V^{bd}_{fi}\left[\delta_{Li}(t_1);L_{Rfi}(t_1;q_1)\right]$ is transferred to the surrounding concrete by bond along the corresponding transfer length $L_{tr,i}(t_1;q_1)$, equal to L_{fi}. For equilibrium to be possible, the progressive value of that force along the corresponding transfer length has to be lower than the concrete tensile fracture capacity. The progressive concrete tensile fracture capacity $V^{cf}_{fi}\left(X^l_i;\alpha;f_{ctm}\right)$ is obtained by: a) spreading the mean tensile strength f_{ctm} over the resulting semi-conical surface with vertex in X^l_i, b) integrating over such surface, and c) projecting in the laminate direction, where $O^l_i X^l_i$ is the reference axis along the i-th strip available bond length. For the simplified case of strips orthogonal to the crack and no interaction between adjacent strips, the progressive value of the concrete tensile fracture capacity is given by: $V^{cf}_{fi}\left(X^l_i;\alpha;f_{ctm}\right)=\pi/2\cdot f_{ctm}\cdot tg^2\alpha\cdot\left(X^l_i\right)^2$, where α is the angle between the axis and generatrices of the semi-conical surface (Fig. 5e). If the progressive value of the force transferred to the surrounding concrete $V^{bd}_{fi}\left(x^{tr}_i\right)$ along the transfer length, scanned from the loaded end inwards, exceeds the corresponding progressive value of the concrete fracture capacity $V^{cf}_{fi}\left(X^l_i\right)$, concrete fractures. Then, a semi-conical crack forms, whose vertex V_c is located at the innermost point where $V^{bd}_{fi}\left(x^{tr}_i\right)\geq V^{cf}_{fi}\left(X^l_i\right)$.

For the example of Fig. 5, since equilibrium is not attained yet, it is necessary to iterate. The force transfer mechanism moves inwards to the still embedded part of the laminate $L_{Rfi}(t_1;q_2)$ (Fig. 5b) where again, if the progressive value of the force transferred exceeds the concrete tensile fracture capacity, another semi-conical crack forms and a further concrete semi-conical slice detaches from the inner concrete. This process continues until, under the imposed slip, $\delta_{Li}(t_1)$, equilibrium is reached within concrete (Fig. 5c). At the next imposed slip increments, that process recurs and other semi-conical cracks might form as shown in Fig. 5d,e where progressively thicker lines represent the

force transferred by bond to concrete along the corresponding transfer length for increasing imposed slips.

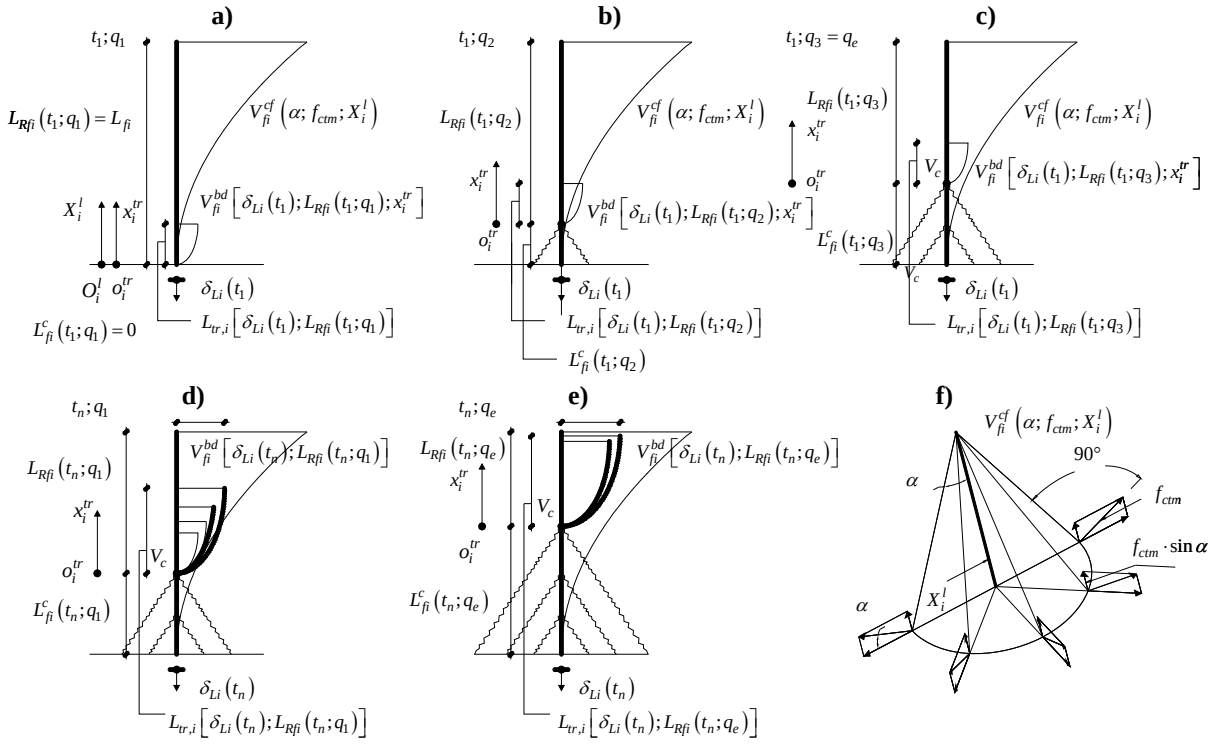

Figure 5: Formation of concrete semi-conical fracture surfaces and iterative search for equilibrium: (a) first q_1, (b) second q_2 and (c) third iteration q_e, for the for the first load step t_1; (d) first q_1 and (e) second iteration q_2, for the t_n load step; (f) concrete fracture capacity evaluation.

It can happen that, for a certain value of the imposed slip, after formation of a series of concrete semi-conical coronas, the residual embedded length fails by debonding (Fig. 6a). This justifies the possibility of having a mixed shallow-cone-plus-debonding failure mode as found in the case of adhesive anchors [11]. Moreover, and especially for short available bond lengths, the process of formation of consecutive concrete semi-conical slices can reach the free end so that, at ultimate, a concrete semi-cone results, whose height corresponds to the initial available bond length (Fig. 6b).

It arises that the spacing between consecutive semi-conical cracks also depends on the CDC angle increment $\dot{\gamma}$. If, for a given load step $\gamma(t_n)$ equilibrium is possible for the i-th strip, its contribution is equal to the minimum between the bond transferred force $V_{fi}^{bd}(t_n;q_e)$ and the strip tensile rupture $V_{fi}^{tr}=a_f\cdot b_f\cdot f_{fu}$. On the contrary, if for concrete surrounding the i-th strip equilibrium is not possible, its contribution is given by its concrete fracture capacity $V_{fi}^{cf}(t_n;q_n)$ calculated in the innermost point of the current transfer length, i.e., $V_{fi}^{cf}\left[L_{fi}^c(t_n;q_n)+L_{tr,i}(t_n;q_n)\right]$. At the same time if, at the previous load step, the i-th strip had reached its ultimate state, for the current load step, its contribution to shear strength is assumed as null.

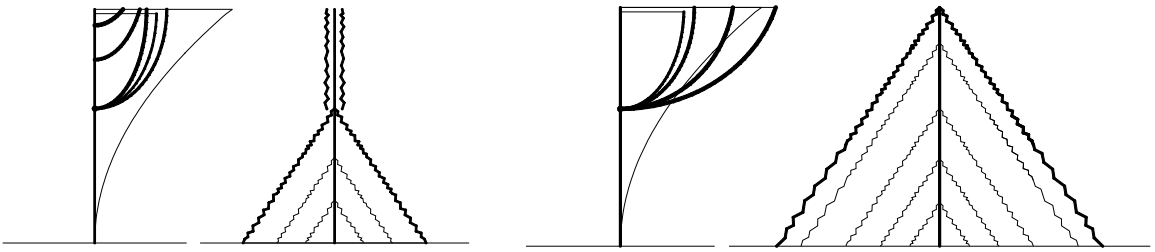

a) b)

Figure 6: Variation of force transferred by bond to the surrounding concrete for increasing values of imposed slip (left) and configuration of the NSM strip at ultimate (right) for: mixed shallow semi-cone plus debonding failure mode (a) and semi-conical tensile fracture (b).

2.3 Bond behaviour and debonding

Referring to a typical push pull test and taking into consideration equilibrium, compatibility and constitutive laws of the intervening materials [9], the following governing differential equation is obtained:

$$\frac{d^2\delta}{dx^2} - \tau\left[\delta(x)\right]\cdot J_1 = 0 \tag{2}$$

with:

$$J_1 = \frac{L_p}{A_f}\cdot\left(\frac{1}{E_f} + \frac{A_f}{A_c\cdot E_c}\right) \tag{3}$$

where: E_c is the concrete Young's Modulus obtained by literature relationships from f_{cm}; A_f and A_c are the cross sectional area of the strip and concrete specimen, respectively, and L_p is the effective perimeter equal to $L_p = 2\cdot b_f + a_f$. Eq. 2 is then solved referring to an infinite bond length and for the different phases of bond.

Once the bond problem has been solved for an infinite bond length, the value of: transfer length $L_{tr,i}\left(L_{Rfi};\delta_{Li}\right)$, corresponding force $V_{fi}^{bd}\left(L_{Rfi};\delta_{Li}\right)$ transferred by bond for an imposed slip δ_{Li} and its progressive value along the transfer length $V_{fi}^{bd}\left(L_{Rfi};\delta_{Li};x_i^{tr}\right)$ can be determined for any value of the resisting bond length L_{Rfi} considering debonding propagation as a constant "wave" progressing from the loaded end inwards, towards the free extremity of the NSM strip. For the sake of brevity, all of the analytical details are herein omitted but can be found elsewhere [9].

2.4 Concrete tensile fracture and interaction among laminates

If the simplifying assumption of large spacing among strips is abandoned, NSM strips interact with each other and the relevant semi-conical fracture surfaces overlap. In the most general case in which both the interaction between adjacent strips cannot be neglected, and when they are not orthogonal to the crack plane, the calculation of the progressive value of the concrete tensile fracture capacity $V_{fi}^{cf}\left(X_i^l;t_n;q_n\right)$ becomes more complicate. A closed-form algorithm is adopted to calculate that capacity as a function of the several parameters involved i.e.: $V_{fi}^{cf}\left(X_i^l;t_n;q_n\right) = f\left[\, f_{ctm};\alpha;\theta;\beta;s_f;h_w;b_w;L_j^c\left(t_n;q_n\right)\forall\, j=1,..N_f \,\right]$. Further details can be found elsewhere [5,8].

3 APPRAISAL OF THE PROPOSED MODEL

The two beams whose experimental results [3] are herein adopted for a preliminar appraisal of the validity of the proposed model, labeled 2S-4LI45 and 2S-7LI45, present CFRP strips disposed at 45 degrees with respect to the beam axis and a spacing of 257 and 157 mm, respectively. Those two beams are also characterized by the following common mechanical and geometrical parameters: $b_w = 180.0\,\text{mm}$; $h_w = 300.0\,\text{mm}$; $f_{cm} = 18.6\,\text{MPa}$; $f_{fu} = 2952.0\,\text{MPa}$; $E_f = 166.6\,\text{MPa}$; $a_f = 1.4\,\text{mm}$; $b_f = 10.0\,\text{mm}$. The parameters characterizing the local bond stress-slip relationship, being the average values of those obtained in a previous investigation [9], are: $\tau_0 = 2.0\,\text{MPa}$; $\tau_1 = 20.1\,\text{MPa}$; $\tau_2 = 9.0\,\text{MPa}$; $\delta_1 = 0.07\,\text{mm}$; $\delta_2 = 0.83\,\text{mm}$; $\delta_3 = 14.1\,\text{mm}$. For the CDC angle, θ, is was assumed the value of 45°. The value of α is assumed equal to $28.5°$ that is also the average of the values obtained from a previous investigation [5] but, in this respect, further investigations are deemed as necessary. The two parameters characterizing the loading process are: $\dot{\gamma} = 0.01°$ and $\gamma_{\max} = 1.5°$. Concrete average tensile strength is calculated from the average compressive strength by means of literature formulae [12].

The analytical results along with the experimentally recorded value of the NSM shear strengthening contribution are plotted in Fig. 7 and the resulting crack scenario for each of the three geometrical configurations is plotted in Figs. 8 and 9. The trace of the semi-conical cracks on the web face is shown together with the value of the angle γ in correspondence of which those cracks occurred.

As expected, up to the maximum contribution of the NSM strips, an increase on the number of strips that are bridging the CDC results in a higher ratio between the NSM shear strengthening contribution and the CDC opening angle. However, due to the group effect (see Fig. 9), the increase in terms of the maximum contribution of the NSM strips for the beam shear resistance, with the increase of the number of strips, was not so high as was registered experimentally (compare graphs of Fig. 7a and 7b). This deficient prediction might be related with the fact of have assumed a constant inclination for the CDC. In fact, experimental tests and analytical models are showing that the inclination of the CDC decreases with the increase of the FRP shear strengthening ratio [13, 14], which under the framework of the model developed in the present work, result in higher values for the maximum contribution of the NSM strips. The influence of the CDC inclination, as well as of other relevant parameters, on the effectiveness of the NSM strengthening technique for the shear resistance of concrete beams will be explored in future publications, using the present model.

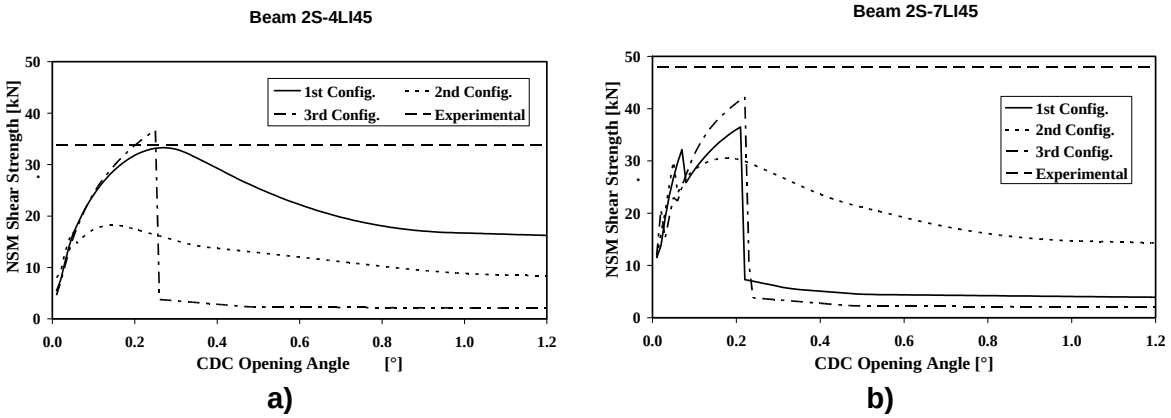

Figure 7: Comparison between analytical predictions and experimental recordings: beam 2S-4LI45 (a) and 2S-7LI45.

For the cases herein analyzed, due to the concrete low strength, strip rupture never occurs. Every

strip is characterized by an initial fracture of the surrounding concrete.

After that, in some cases the strip can fail, since the semi-conical concrete fracture reaches the free end, which generally happens for the first load steps and for the smaller available bond lengths. Those failures, as for the 2nd strip of the first configuration of beam 2S-4LI45 at step $\gamma = 0.01°$ (Fig. 8) or for the 1st strip of the 2nd configuration of beam 2S-7LI45 (Fig. 9), are not evident in the graph since, at that stage, the longer strips' contribution is increasing and much higher in percentage terms. When concrete fracture reaches the strip inner tip at a higher step, as for the 3rd strip of the 1st configuration of beam 2S-7LI45 at $\gamma = 0.07°$, the sudden drop of strength is much more evident (Fig. 7b).

In other cases, the sudden drop of strength is due to the mixed failure of one of the strips, as occurs for the 2nd strip of the 1st configuration of beam 2S-7LI45 at step $\gamma = 0.22°$ *i.e.*: due to further semi-conical crack occurred, the imposed end slip being constant, the resisting bond length abruptly reduces and the bond transferred force reduces in turn. Anyway, after that brittle reduction of strength, since that strip does not undergo any further concrete cracking-induced reduction, bond transferred force goes on decreasing gradually, as can be gathered, for instance, from the graph of 1st configuration of beam 2S-7LI45.

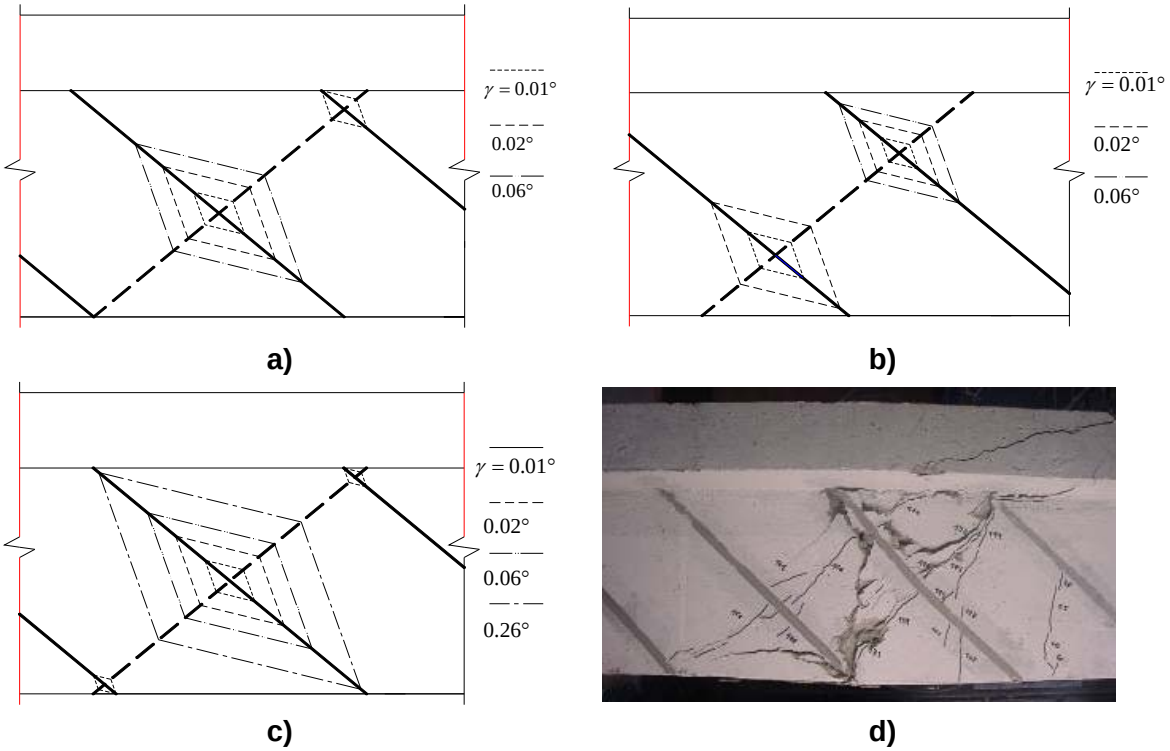

Figure 8: Beam 2S-4LI45: simulated ultimate state for the (a) first, (b) second and (c) third geometrical configuration analyzed; (d) post test picture.

When after the initial shallow semi-conical cracking, the resisting bond length is still a high amount of the initial available bond length, and it keeps on being, at each step, systematically larger than the corresponding value of the necessary transfer length, determined, this latter, thinking of an infinite resisting bond length [9], the strip behavior is mainly governed by bond mechanism. Since this latter is characterized by a gradual variation of capacity, according to the modeling strategy herein adopted, the overall response results smooth as well, see, for instance, what happens with the 1st configuration of beam 2S-4LI45 or the 2nd of beam 2S-7LI45.

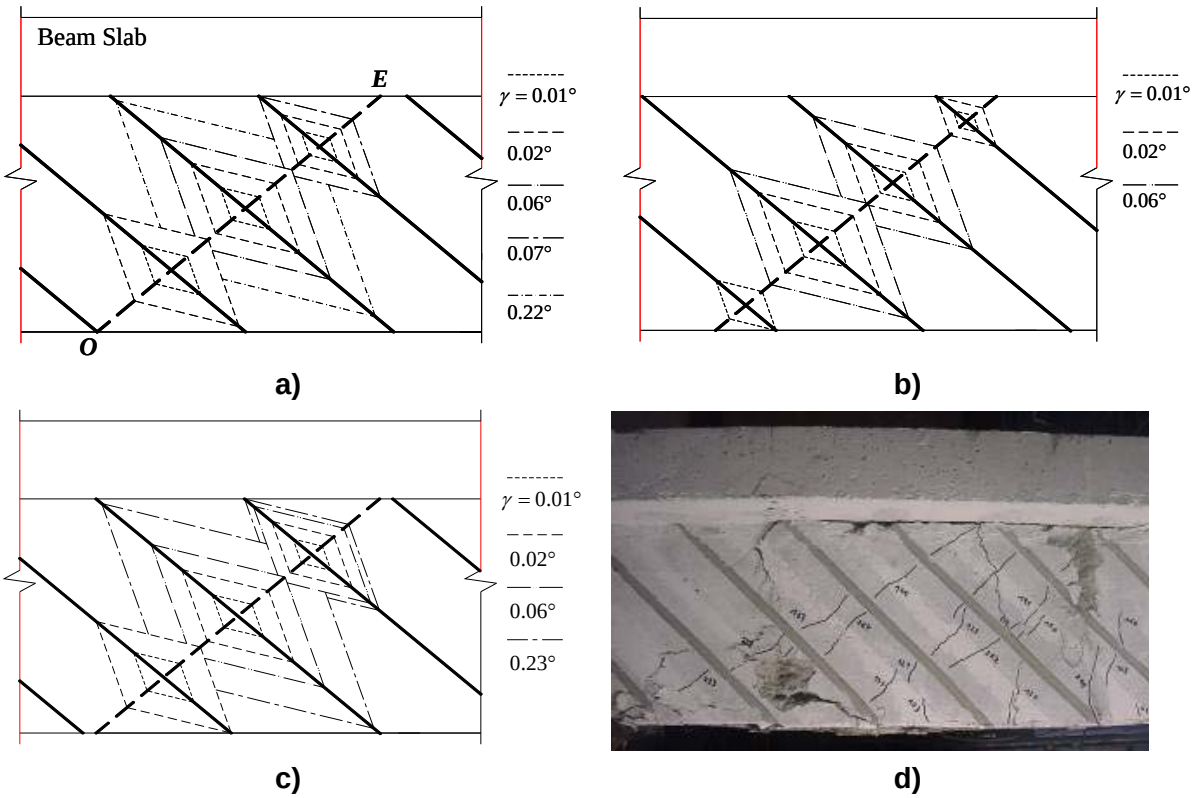

Figure 9: Beam 2S-7LI45: simulated ultimate state for the (a) first, (b) second and (c) third geometrical configuration analyzed; (d) post test picture

4 CONCLUSIONS

The upgraded version of the analytical model recently developed to predict the NSM FRP strips shear strength contribution to RC beams was presented along with its preliminary appraisal. Despite the necessity to better calibrate some parameters such as the angle between the axis and generatrices of the semi-conical fracture surface and the inclination of the critical diagonal crack, the results show such model is capable of simulating correctly the physical behavior of a group of FRP strips glued in the cover of RC beams lateral faces.

The maximum strength predictions are deemed satisfactory enough especially if it is taken into consideration that: the model neglects the softening behavior of concrete in tension, the high scatter affecting concrete tensile strength and, on the contrary, the simplified and indirect way in which it was herein calculated.

This model can be conveniently applied to evaluate the influence of each of the intervening parameters on the maximum shear strength contribution provided by system of FRPs glued in the cover of RC beams in order to get useful information for designers.

At the same time, such modeling strategy can be conveniently simplified into a closed form design equation to be used by practitioners interested in the application of such a front-line and promising strengthening technique.

ACKNOWLEDGEMENTS

The authors of the present work wish to acknowledge the support provided by the "Empreiteiros Casais", S&P®, degussa® Portugal, and Secil (Unibetão, Braga). The study reported in this paper forms a part of the research program "SmartReinforcement – Carbon fibre laminates for the strengthening and monitoring of reinforced concrete structures" supported by ADI-IDEIA, Project nº 13-05-04-FDR-00031. Also, this work was carried out under the auspices of the Italian DPC-ReLuis Project (repertory n. 540), Research Line 8, whose financial support is greatly appreciated.

REFERENCES

[1] S.J.E. Dias, J.A.O. Barros, "NSM CFRP laminates for the shear strengthening of T section RC beams", 2nd International fib Congress, Naples, Italy, id 10-58, (2006).
[2] L. De Lorenzis, A. Rizzo, "Behaviour and capacity of RC beams strengthened in shear with NSM FRP reinforcement", 2nd Int. fib Congress, Naples-Italy, June 5-8, PAPER ID 10-9 IN CD, (2006).
[3] S.J.E. Dias, V. Bianco, J.A.O. Barros, G. Monti, "Low strength concrete T cross section RC beams strengthened in shear by NSM technique", Workshop-Materiali ed Approcci Innovativi per il progetto in zona sismica e la mitigazione della vulnerabilità delle strutture, University of Salerno, Italy, 12-13 February 2006.
[4] V. Bianco, J.A.O. Barros, G. Monti, "A new approach for modeling the NSM shear strengthening contribution in reinforced concrete beams", FRPRCS-8, University of Patras, Greece,16-18 July, ID 8-12, (2007).
[5] V. Bianco, J.A.O. Barros, G. Monti, "Shear strengthening of RC beams by means of NSM laminates: experimental evidence and predictive models", Technical Report 06-DEC/E-18, Dep. Civil Eng., School Eng. University of Minho, Guimarães- Portugal (2006).
[6] V. Bianco, J.A.O. Barros, G. Monti, "Influence of the concrete mechanical properties on the efficacy of the shear strengthening intervention on RC beams by NSM technique", Asia-Pacific Conference on FRP in structures, University of Hong Kong, China,12-14 December (2007).
[7] G. Monti, M.A. Liotta, "Tests and design equations for FRP-strengthening in shear", International Journal of construction and building materials, 21, 799-809, Elsevier, September (2006).
[8] V. Bianco, "Shear strengthening of RC beams by means of NSM FRP strips: experimental evidence and analytical modeling", PhD Thesis, Dept. of Structural Engrg. and Geotechnics, Sapienza University of Rome, (in preparation).
[9] V. Bianco, J.A.O. Barros, G. Monti, "Shear strengthening of RC beams by means of NSM strips: a proposal for modeling debonding", Technical Report 07-DEC/E-29, Dep. Civil Eng., School Eng. University of Minho, Guimarães- Portugal 2007.
[10] J.A.O. Barros, J.M. Sena Cruz, "Bond between near-surface mounted CFRP laminate strips and concrete in structural strengthening", Journal of Composites for Construction, 8(6), p. 519-527, (2004).
[11] R.A. Cook, J. Kunz, W. Fuchs, R.C. Konz, "Behaviour and Design of single adhesive anchors under tensile load in uncracked concrete", ACI Structural Journal, Vol. 95, No.1, January/February, PP. 9-26 (1998).
[12] CEB-FIP Model Code 90, Bulletin d'information N° 213/214, final version printed by TH. Telford, LONDON, (1993; ISBN 0-7277-1696-4; 460 pages).
[13] A. Aprile, A. Benedetti, "Coupled flexural-shear design of R/C beams strengthened with FRP", *Composites: Part B Engineering*, 35, 1–25 (2004).
[14] *Dias, S.J.E.; Barros, J.A.O.,* "Shear strengthening of T cross section reinforced concrete beams by near surface mounted technique", accepted to be published in the *Journal of Composites for Construction* (2008).